JOINT CONFERENCE PROCEEDINGS
7th International Conference on Urban Earthquake Engineering (7CUEE) &
5th International Conference on Earthquake Engineering (5ICEE)
March 3-5, 2010, Tokyo Institute of Technology, Tokyo, Japan

2- AND 3-D BLIND ANALYSES OF FULL-SCALE 5-STORY BUILDING WITH VISCOUS DAMPERS

Tadamichi Yamashita[1], Jun Kawabata[1], Masayuki Ninomiya[2], Norikazu Sakaba[2] and Yukimori Yanagawa[3]

1) Structural Design Department, Osaka Office, Kozo Keikaku Engineering Inc., Japan
2) Structural Design Department, Tokyo Office, Kozo Keikaku Engineering Inc., Japan
3) Disaster Prevention Consulting Department, Kozo Keikaku Engineering Inc., Japan

E-mail: tad-yamashita@kke.co.jp, jun@kke.co.jp, mninomiy@kke.co.jp, sakaba@kke.co.jp, yanagawa@kke.co.jp

Abstract: A blind analysis contest has been conducted in conjunction with full-scale 5-story building specimens with two damper types in March 2009 at the E-Defense shake-table facility. The purpose of the contest is to stimulate development of computational methods and efficient modeling techniques for steel frame buildings with various dampers. The building shaking-table was tested repeatedly, inserting and replacing each of four damper types, i.e., steel damper, oil damper, viscous damper, and viscoelastic damper. This blind analysis contest is categorized by the combination of two damper types (steel and viscous damper) and two analysis types (3-D and 2-D analysis) into four categories. Authors' group participated in all categories, and won first place in the 3-D (viscous damper) and 2-D (viscous damper) categories. In this report, we present the methods of modeling and the result of seismic analysis in these two winning categories.

1. INTRODUCTION

Founded as a structural design firm in 1956, Kozo Keikaku Engineering Inc., where the authors work at, has expanded its line of business to a variety of fields in structural design as well as software development that helps design flow. We have entered this contest in all categories, aiming to serve test cases for RESP-F3T (our newly-developed 3D analysis software of general purpose) at the same time. Our team has won first place in 2 categories that are assigned with viscous dampers in steel building in 3-D and 2-D model. In this paper are described the analysis models and results of seismic response simulations in these 2 award-winning categories as well as the technical tips for further accuracy improvement.

2. MODEL OF FIVE-STORY STEEL FRAME

We created the detailed structural model for the blind analysis contest using three approaches of modeling principally, such as modeling the steel frame building, modeling the viscous damper including brace and other members, and modeling the viscous damping of steel frame itself (without viscous dampers). (Figure 2.1) First, the steel frame building and the viscous damper system were modeled based upon the design specification and experimental result of the viscous damper distributed by National Research Institute for Earth Science and Disaster Prevention (NIED). The viscous damping of steel frame was modeled by our original approach. Instead of using the typical damping model, we created a model by ourselves, evaluated it and then employed it as analysis model.

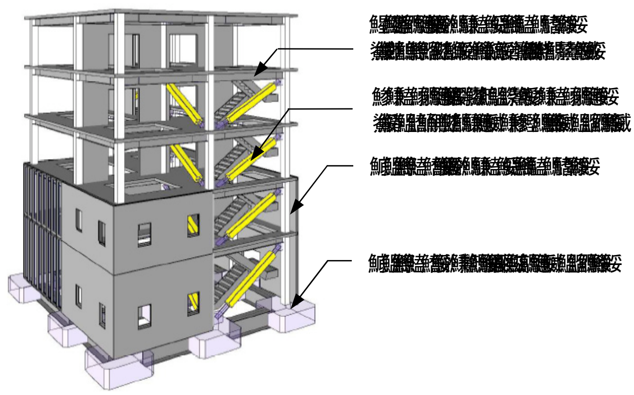

Figure 2.1 Structural Model (3 – D analysis)

Weight appraisal of the steel building (except the viscous damper systems) was determined by the calculation based on the design specification, referring to the figures disclosed by NIED, which are shown in the parenthesis in the table below. (Table 2.1)

Table 2.1 Comparison of the Weight Distribution

[illegible]

[illegible]	[illegible]	[illegible]	[illegible]	[illegible]	[illegible]	[illegible]
[illegible]	[illegible]	[illegible] / [illegible]	[illegible]	[illegible]	[illegible]	[illegible]
[illegible]	[illegible]	[illegible] / [illegible]	[illegible]	[illegible]	[illegible]	[illegible]
[illegible]	[illegible]	[illegible] / [illegible]	[illegible]	[illegible]	[illegible]	[illegible]
[illegible]	[illegible]	[illegible] / [illegible]	[illegible]	[illegible]	[illegible]	[illegible]
[illegible]	[illegible]	[illegible] / [illegible]	[illegible]	[illegible]	[illegible]	[illegible]

[illegible]

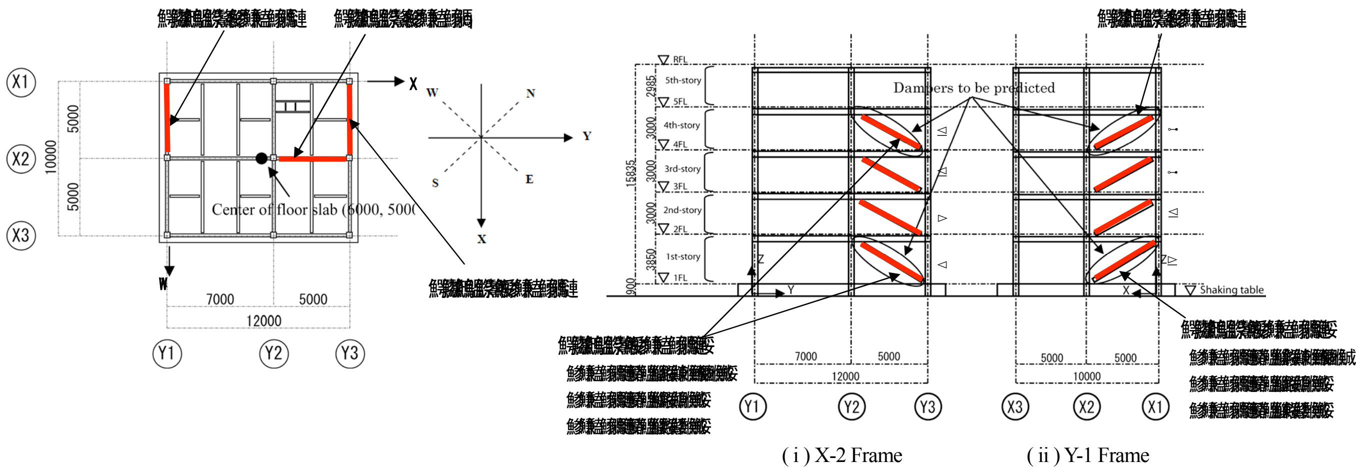

(a) Horizontal Plan (b) Elevational Plan

Figure 2.2 5-Story Steel Building with Viscous Dampers

Table 2.2 Modulus of Eccentricity for 5-Story Steel Building

[illegible]	[illegible]	[illegible]	[illegible]	[illegible]	[illegible]	[illegible]
[illegible]	[illegible]	[illegible]	[illegible]	[illegible]	[illegible]	[illegible]
[illegible]	[illegible]	[illegible]	[illegible]	[illegible]	[illegible]	[illegible]
[illegible]	[illegible]	[illegible]	[illegible]	[illegible]	[illegible]	[illegible]
[illegible]	[illegible]	[illegible]	[illegible]	[illegible]	[illegible]	[illegible]
[illegible]	[illegible]	[illegible]	[illegible]	[illegible]	[illegible]	[illegible]

' I`o`mdrd Rdhrlhb Cdhrfm Hmcdw 9 Qdw∗Qdx(

Table 2.3 Modeling and Analysis Method in Each Category

[illegible]	[illegible]	[illegible]
[illegible]	[illegible]	[illegible]
[illegible]	[illegible]	[illegible]
[illegible]	[illegible]	[illegible]
[illegible]	[illegible]	[illegible]

Table 2.1 shows the weight distribution by member type. Compared to the figures we calculated based upon the design specification, the figures disclosed by NIED have small discrepancies but are all higher than the calculated ones with the numerical error of approximate 2 % in every story.

The steel building is installed with viscous dampers as shown in Figure 2.2. The modeling technique of the steel building alone shall be described in this chapter. (Modeling the viscous damper system is illustrated in the following chapter.)

- Model of Steel Elements
  As for the tension strength of columns and girders, yield strength of each member was defined based on the distributed result of material experiment.
- Model of Concrete
  The compressive strength of concrete was specified with the experimental result obtained 90 days after casting. (Young modulus: $3.004 \times 10^{4}\,\mathrm{N/mm^{2}}$)
- Composite Beam Model
  Assuming the girder as a composite beam with slab, its section modulus and neutral axis were calculated in accordance with "***Design Recommendations for Composite Constructions***" by Architectural Institute of Japan. The effective width of slabs was determined with reference to ***Standard for Structural Calculation of Reinforced Concrete Structures***.
- Description of Member Model
  Both columns and girders were modeled as beam elements and the girder haunch was modeled as rigid zone.
- Details of the Model of Column Hinge
  M-N correlation was applied to the hinge area of each member.
- Column-Base Model
  The column bases were built as fiber models with rotational springs fully fixed.
- Model of Slabs
  Assumption of rigid floor was applied for slab modeling.

After creating the model with the aforesaid specifications for each material, the modulus of eccentricity were obtained for steel frame building without damper systems. (Table 2.2) The eccentricity of strength was not calculated, assuming that the steel frame would stay mostly within the elastic region. As shown in Table 2.2, the eccentricity ratio of each story of the steel frame has the maximum value of 0.043 on the 1st story (X-direction) and 0.02 ~ 0.04 on the other stories in each direction. Having these figures, we determined that the steel building for this analysis contest scarcely has eccentricity impact. Therefore, the structural models for 2-D and 3-D categories of this blind analysis contest were built in 3-D, creating 2-D models from 3-D in YZ-plane: Y-direction, Z-direction, and X-rotation (rotation with respect to X-axis). The analysis model and method are represented in Table 2.3.

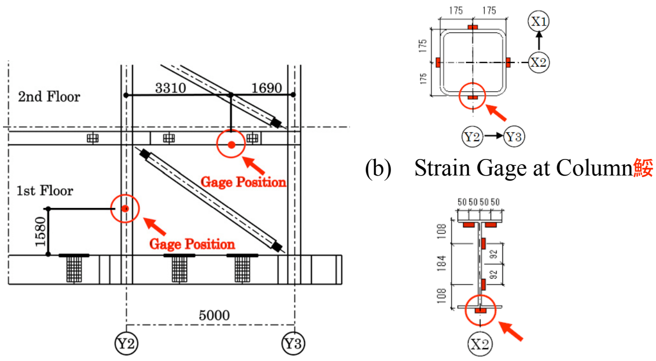

(a) X2-Elevation綏 (b) Strain Gage at Column綏 (c) Strain Gage at Girder綏

Figure 2.3 Specified Point of Strain Frame綏

The column strain was calculated from the axial strain and bending strain. Obtaining the axial strain from the axial force of column, and the bending strain by calculating the bending moment at the strain gage point shown in Figure 2.3 based on the bending moment of the base and top of column, the column strain was gained by summing those values dynamically.

As shown in Figure 2.3, specifying the strain locations at girder as nodal points in the analysis model, the girder strain was calculated from the axial force and bending moment at those specified nodal points. The axial strain was calculated from axial cross-sectional area of girder with consideration of the effective width of slab when it has compressive axial force, while it was calculated from the axial cross-section of the girder only when it has tensile axial force. The bending strain was calculated respectively for each neutral axis of positive and negative moment, and thus the section modulus was obtained.

3. MODEL OF VISCOUS DAMPERS

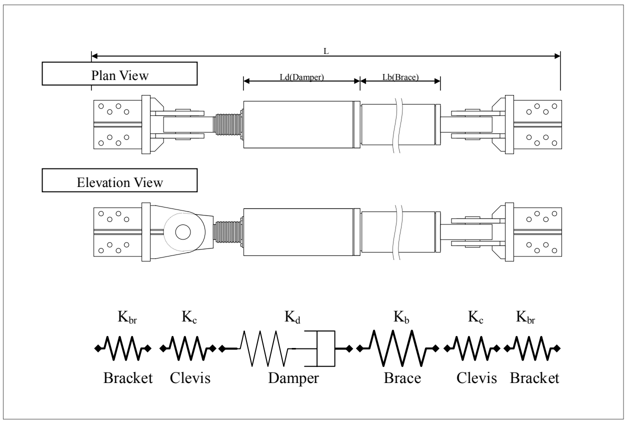

Figure 3.1 Model of Viscous Damper (Maxwell Model)

The viscous damper that is employed for this blind analysis contest is called "Non-Linear Maxwell Model", whose dashpot exerts damping force proportional to the power of the velocity, α. (Figure 3.1)

Table 3.1 Characteristics of Maxwell Model (Non-Linear)

[illegible]	[illegible]	[illegible]	[illegible]	[illegible]
[illegible]	[illegible]	[illegible]	[illegible]	[illegible]
	[illegible]	[illegible]	[illegible]	[illegible]
	[illegible]	[illegible]	[illegible]	[illegible]
	[illegible]	[illegible]	[illegible]	[illegible]
[illegible]	[illegible]	[illegible]	[illegible]	[illegible]
	[illegible]	[illegible]	[illegible]	[illegible]
	[illegible]	[illegible]	[illegible]	[illegible]
	[illegible]	[illegible]	[illegible]	[illegible]

While the coefficient of damping (Cd) of the viscous damper installed in the steel building and α, the power of the velocity are provided by its manufacturer, and the stiffness of the viscous damper (K_d) was determined in reference to the experimental data of the damper alone, we had to conjecture the stiffness of the viscous damper K_d at the coefficient of damping of $C_d = 49$ kN/(mm/s)$^{0.38}$. (Table 3.1) Likewise, another model of viscous damper with coefficient damping value of C_d = 131 kN/(mm/s)$^{0.38}$ was also distributed (but not installed in the building) as a referential data for theorizing the damper stiffness K_d. Based on all of those damper characteristics, the damper stiffness K_d was determined.

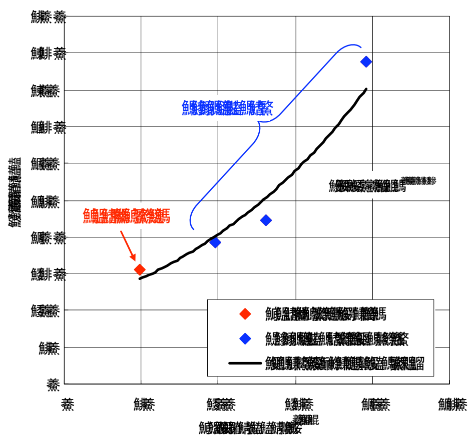

Figure 3.2 C_d綏 K_d Relation of Viscous Dampers

Figure 3.2 represents the correlation between the coefficient of damping C_d and the damper stiffness K_d, referring to the distributed specimen data of the viscous damper. Having no experiments done, the stiffness of the viscous damper K_d at the coefficient of damping of $C_d = 49$ kN/(mm/s)$^{0.38}$ needed to be speculated by the least squares method as shown in Figure 3.2. In this calculation, the stiffness K_d corresponding to the model with the coefficient of damper of C_d = 49 kN/(mm/s)$^{0.38}$ (one without any experimental data) becomes too small when assuming the coefficient of damper C_d and the damper stiffness K_d to have linear relation. Instead, we adopted relation with index function to have variants in curvature, which was K_d = 155 kN/(mm/s).

Table 3.2 Stiffness of Damper, Brace, Clevis and Bracket

[illegible]

[illegible]	[illegible]	[illegible]	[illegible]	[illegible]	[illegible]	[illegible]
[illegible]	[illegible]	[illegible]	[illegible]	[illegible]	[illegible]	[illegible]
	[illegible]	[illegible]	[illegible]	[illegible]	[illegible]	[illegible]
	[illegible]	[illegible]	[illegible]	[illegible]	[illegible]	[illegible]
	[illegible]	[illegible]	[illegible]	[illegible]	[illegible]	[illegible]
[illegible]	[illegible]	[illegible]	[illegible]	[illegible]	[illegible]	[illegible]
	[illegible]	[illegible]	[illegible]	[illegible]	[illegible]	[illegible]
	[illegible]	[illegible]	[illegible]	[illegible]	[illegible]	[illegible]
	[illegible]	[illegible]	[illegible]	[illegible]	[illegible]	[illegible]

The viscous damper is modeled with components coupled in series as shown in Figure3.1. The total stiffness of the viscous damper including brace and other members is calculated using Maxwell equations (Eq 3.1) with the stiffness of the viscous damper alone K_d, the stiffness of the brace K_b, the stiffness of the clevis K_c, and the stiffness of the bracket K_{br}. (Table 3.2)

$$\frac{1}{K_{max\,well}} = \frac{1}{K_d} + \frac{1}{K_b} + 2\frac{1}{K_c} + 2\frac{1}{K_{br}} \qquad (3.1)$$

Since the viscous damper is connected eccentrically from the center line of the girder, the mounting angle was tuned by setting additional nodal points in vertical direction for columns with consideration for eccentric moment. The gusset plate mounted on the damper on steel frame side is connected in series, assessing the stiffness of the plate.

4. SELECTED MODAL DAMPING RATIOS

Table4.1 Periods and Participation Factors for 3-D Model

[illegible]	[illegible]	[illegible]				[illegible]
		[illegible]	[illegible]	[illegible]	[illegible]	
[illegible]	[illegible]	[illegible]	[illegible]	[illegible]	[illegible]	[illegible]
[illegible]	[illegible]	[illegible]	[illegible]	[illegible]	[illegible]	[illegible]
[illegible]	[illegible]	[illegible]	[illegible]	[illegible]	[illegible]	[illegible]
[illegible]	[illegible]	[illegible]	[illegible]	[illegible]	[illegible]	
[illegible]	[illegible]	[illegible]	[illegible]	[illegible]	[illegible]	
[illegible]	[illegible]	[illegible]	[illegible]	[illegible]	[illegible]	
[illegible]	[illegible]	[illegible]	[illegible]	[illegible]	[illegible]	
[illegible]	[illegible]	[illegible]	[illegible]	[illegible]	[illegible]	
[illegible]	[illegible]	[illegible]	[illegible]	[illegible]	[illegible]	
[illegible]	[illegible]	[illegible]	[illegible]	[illegible]	[illegible]	
[illegible]	[illegible]	[illegible]	[illegible]	[illegible]	[illegible]	[illegible]
[illegible]	[illegible]	[illegible]	[illegible]	[illegible]	[illegible]	

[illegible]

The viscous damping model of typical low-rise buildings is stiffness proportional damping. If this model was applied to the steel frame building of this blind analysis contest, the viscous damping would have resulted inevitably in high value for higher modes due to the lack of dynamic interaction with ground. Furthermore, the viscous damping in Z- direction (vertical) for 1st mode needs to be specified at minimum value in order to simulate three directions in X, Y, and Z simultaneously.

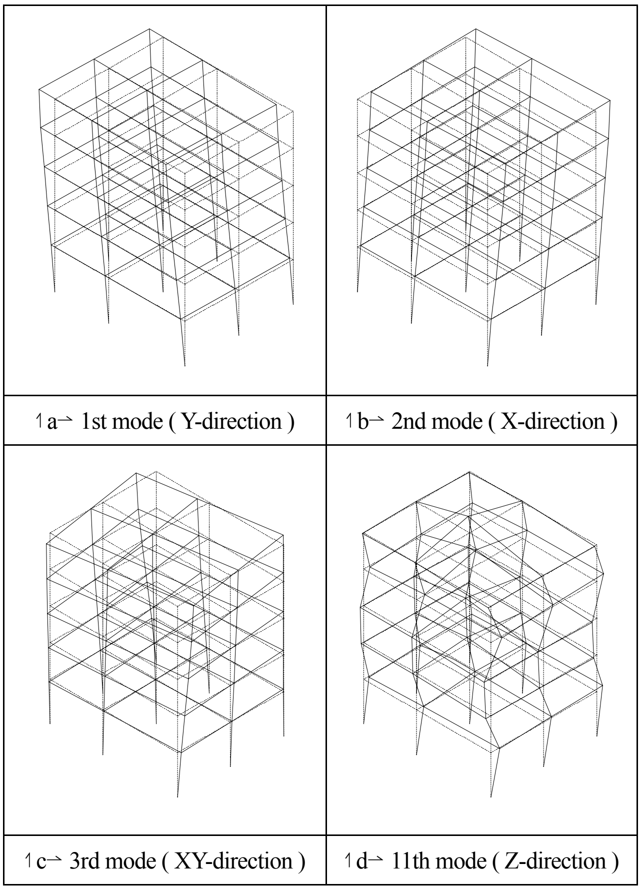

Figure 4.1 Modes of 5-Story Building without Dampers

Therefore, Rayleigh damping model was applied, which is used relatively in common for high-rise buildings to determine the viscous damping for the analysis model.

Assuming the damping matrix to be proportional to a combination of the mass and the stiffness matrices, Eq 4.1 shall be obtained.

$$C = a0 \cdot [M] + a1 \cdot [K] \qquad (4.1)$$

Given Eq 4.1, modal damping ratio (h_n) leads to the following relation between two constants ($a0$, $a1$) and one frequency (ω_n) for Rayleigh damping. (Eq 4.2)

$$h_n = \frac{a0}{2 \cdot \omega_n} + \frac{a1 \cdot \omega_n}{2} \qquad (4.2)$$

Once, the damping constants h_i, h_j regarding the two vibration frequency ω_i, ω_j are specified in Eq 4.2, a set of simultaneous equations is established for invariables $a0$, $a1$. In the other words, damping constants h_i , h_j can be back-calculated by specifying the two constants $a0$, $a1$.

Thus we sought and extracted the constants $a0$, $a1$ that have 3%, 3%, 1% as damping ratio of steel frame itself (without viscous damper) in X, Y, Z in the first mode, using linear programming. (Figure 4.2) The first modal damping ratio for X and Y direction were specified as 3 %, anticipating the high damping effect by the relatively high ratio of the mounted materials (exterior-wall etc) on the steel frame compared to the typical buildings.

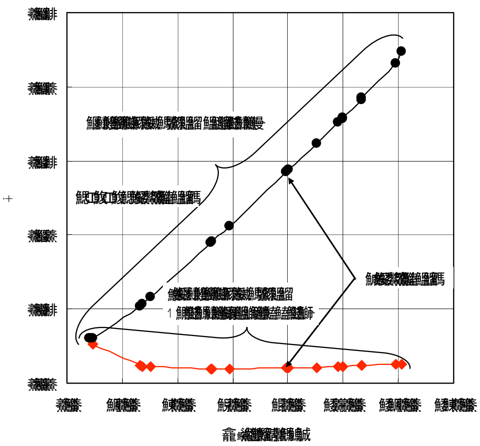

Figure 4.2 Selected by Modal Damping Ratios
(Linear Programming Method)

The value of constants $a0$ and $a1$ are detected and extracted for targeted damping ratio in 2-D and 3-D models by linear programming as shown in Table 4.2.

Table4.2 Target Modal Damping Ratios in Each Category

[illegible]	[illegible]	[illegible]
[illegible]	[illegible]	[illegible]
[illegible]	[illegible]	[illegible]
[illegible]	[illegible]	[illegible]

5. 3 – D PREDICTION OF SEISMIC RESPONSE

Figures 5.2(a) ~ 5.3(b) indicate the maximum response acceleration and the maximum story shear force in X and Y-direction. (Seismic motion inputs were set as 0.4-scale and full-scale wave.)

As can be seen in Figure 5.2(a), the experimental result (dotted line) and the analysis result (solid line) of the maximum response acceleration in X-direction are quite similar when shaken by 0.4-scale and full-scale of Takatori wave. The distribution in Figure 5.2(b) shows that the response acceleration in Y-direction has the same tendency as Figure 5.2(a) regardless to the input levels, however, their experimental results (dotted line) are much higher than the analysis results (solid line) on the top story. Studying the curves of acceleration spectra shown in Figure 5.1(a), the 1st natural period of experimental building is conceivably slightly shorter than the one of analysis model (Y-direction:T = 0.747(s)).

As for the maximum story shear force represented in Figures 5.3(a)(b), the prediction error of the experimental result of maximum response acceleration (dotted line) and the calculated result (solid line) was directly reflected on the analysis value of maximum story shear force, since the figures of weight appraisal had very little differences between the figures NIED distributed and the one that we calculated based on the design specification.

Figures 5.4(a)髓5.5(b) indicate the maximum response displacement and the maximum drift angle in X and Y-direction. (Seismic motion inputs were set as 0.4-scale and full-scale.)

Comparing the maximum response displacement in X and Y-direction with 0.4-scale as in Figures 5.4(a)(b), the analysis result (solid line) is slightly less than the experimental result (dotted line). Nevertheless, the results are quite consistent. On the other hand, the maximum response displacement in X-direction with full-scale input is much higher in analysis (solid line) than experimental result (dotted line). The displacement spectra tendency in Figure 5.1(b) and the speculation in Reference 2) indicate that the 1st natural period of experimental building is shorter than the one of analysis model (X-direction:T=0.724(s)) not only in Y-direction, but also in X-direction.)

Studying the tendency of the displacement spectra, we have noticed that the maximum response displacement in Y-direction is also higher in the region of shorter period than the 1st natural period (Y-direction:T=0.747(s)) of analysis model when shaken in full-scale of Takatori wave. Assuming the 1st natural period of experimental building is around this period range, the discrepancies of experimental result (dotted line) and analysis result (solid line) are quite explainable.

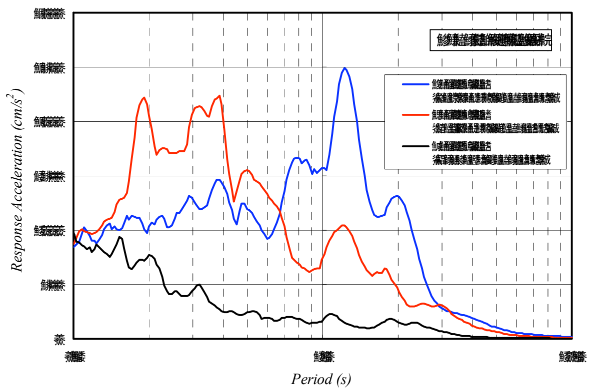

Figure 5.1(a) Acceleration Spectra for the JR Takatori Station Records
(Measured Acceleration of the Shaking-Table)

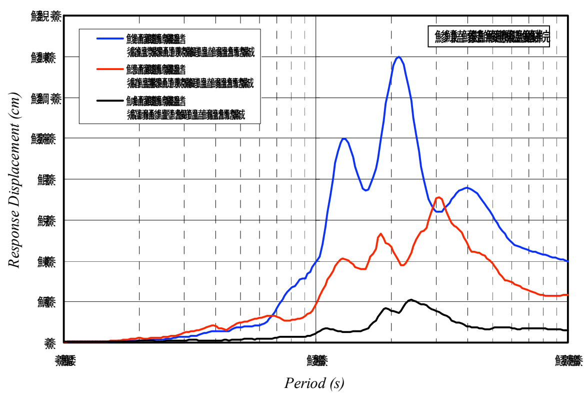

Figure 5.1(b) Displacement Spectra for the JR Takatori Station Records
(Measured Acceleration of the Shaking-Table)

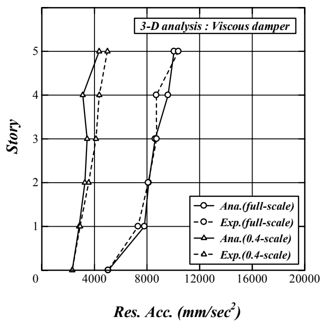

Figure 5.2(a) Maximum Response Acceleration in X-Direction

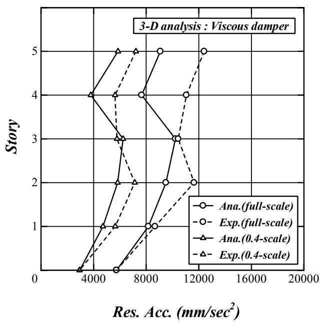

Figure 5.2(b) Maximum Response Acceleration in Y-Direction

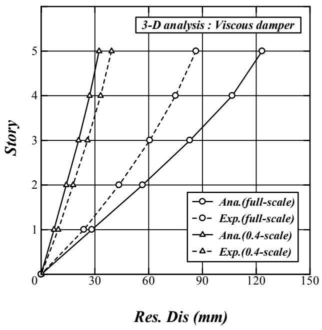

Figure 5.4(a) Maximum Response Displacement in X-Direction

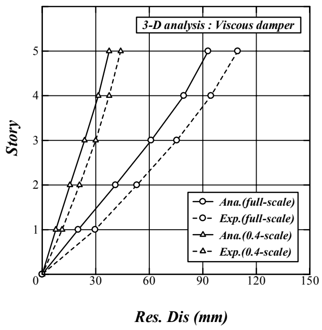

Figure 5.4(b) Maximum Response Displacement in Y-Direction

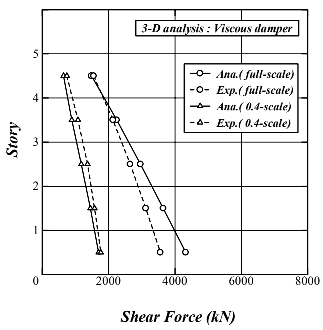

Figure 5.3(a) Maximum Story Shear Force in X-Direction

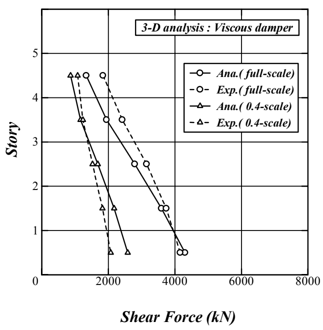

Figure 5.3(b) Maximum Story Shear Force in Y-Direction

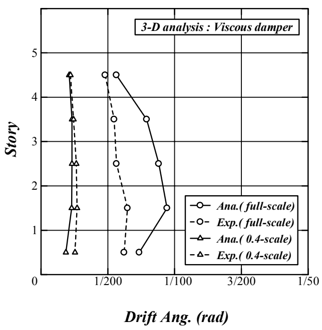

Figure 5.5(a) Maximum Drift Angle in X-Direction

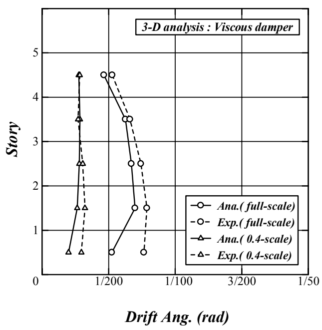

Figure 5.5(b) Maximum Drift Angle in Y-Direction

Presuming that the 1st natural period of experimental building is shorter than the one of analysis model, the consistency of experimental result (dotted line) and analysis result (solid line) in maximum response acceleration as well as maximum response displacement for 0.4-scale of Takatori wave shown in Figures 5.2(a)(b) and Figures 5.4(a)(b) indicate the damping ratio of the steel frame itself (without dampers) has been specified slightly too high and it needs to be specified for each input level respectively.

The maximum drift angle shown in Figures 5.5(a)(b) have mostly the same prediction error as the maximum response displacement in the experimental result (dotted line) and the analysis result (solid line). The maximum drift angle for full-scale of Takatori wave, especially, has very little discrepancy between the experimental result on 1st story and the one immediately upper 1st story (2nd story) compared with the analysis results. Considering above and the fact that the story height of 1st story is taller than the other stories, the shear deformation ratio can be relatively high as a consequence of the loose connection of the pin joint at both edges of dampers, which, in fact, is reported in References 2) and 3).

Figures 5.6(a) ~ 5.9(b) show relations between the axial force and deformation of the viscous dampers that installed on the 1st and 4th stories in X-2 frame and Y-1 frame as shown in Figure 2.2. (Seismic motion inputs were set as 0.4-scale and full-scale of Takatori wave.)

As can be seen in Figures 5.6(a) ~ 5.7(b), the relation of axial force and deformation of dampers installed on the frames in X and Y-directions for 0.4-scale of Takatori wave is quite consistent in the experimental result (dotted line; envelop region) and the analysis result (solid line; Hysteresis Loop), that is to say, the simulation illustrates the experimental outcome with high accuracy.

Looking at Figures 5.8(a) ~ 5.9(b), the relation of axial force and deformation of dampers installed on the frames in X and Y-directions for full-scale of Takatori wave has some larger analysis deformations (solid line) in X-direction than experimental deformations (dotted line), yet, the axial force of dampers are simulated fairly accurately. Moreover, despite the prediction error of analysis and experiment on 1st story, the relation between axial force and deformation of dampers in Y-direction is accurately calculated for the dampers on 4th story.

Table 5.1 Maximum Axial Strain at Column and Girder

[illegible]

[illegible]	[illegible]	[illegible]	[illegible]
[illegible]	[illegible]	[illegible] [illegible]	[illegible] [illegible]
	[illegible]	[illegible]	[illegible]
[illegible]	[illegible]	[illegible]	[illegible]
	[illegible]	[illegible]	[illegible]

[illegible]

Figures shown in Table 5.1 are the respective strain values of columns and girders at the gage point specified in Figure 2.3. (Seismic inputs were set as 0.4-scale and full-scale of Takatori wave.) The values of column strain in 3-D analysis shown in Table 5.1 include modifications in this paper (modified the miscalculation by data processing of time historical response analysis).

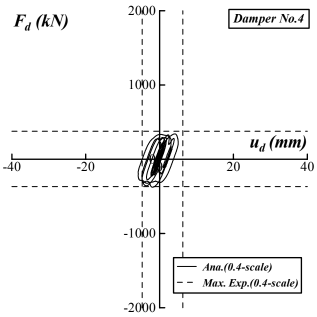

Figure 5.6(a) Force - Deformation Relation of Viscous Damper for 0.4-Scale Wave (1F:X-Direction)

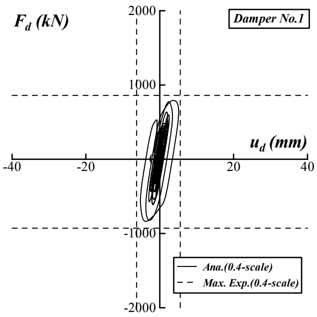

Figure 5.6(b) Force - Deformation Relation of Viscous Damper for 0.4-Scale Wave (1F:Y-Direction)

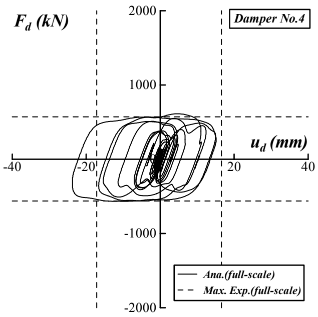

Figure 5.8(a) Force - Deformation Relation of Viscous Damper for Full-Scale Wave (1F:X-Direction)

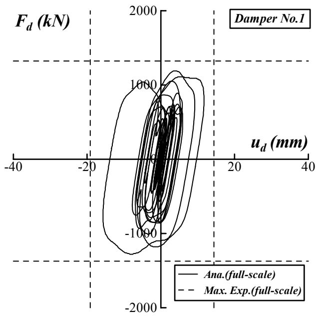

Figure 5.8(b) Force - Deformation Relation of Viscous Damper for Full-Scale Wave (1F:Y-Direction)

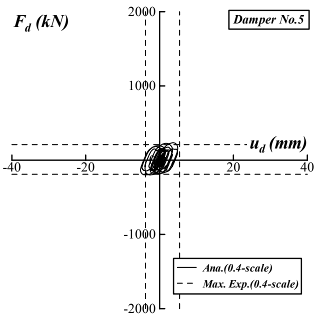

Figure 5.7(a) Force - Deformation Relation of Viscous Damper for 0.4-Scale Wave (4F:X-Direction)

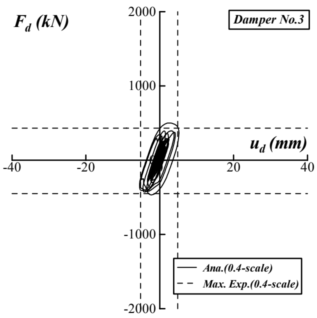

Figure 5.7(b) Force - Deformation Relation of Viscous Damper for 0.4-Scale Wave (4F:Y-Direction)

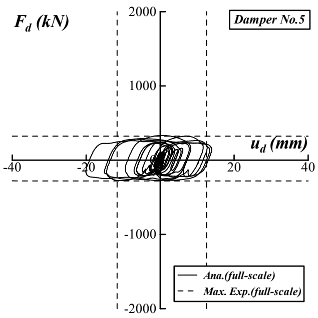

Figure 5.9(a) Force - Deformation Relation of Viscous Damper for Full-Scale Wave (4F:X-Direction)

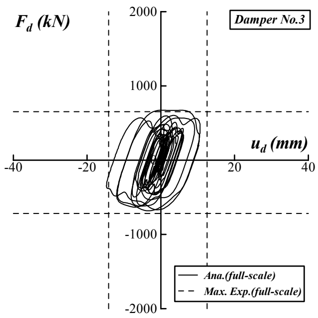

Figure 5.9(b) Force - Deformation Relation of Viscous Damper for Full-Scale Wave (4F:Y-Direction)

The results in Table 5.1 indicate approximate 10-40% errors in axial strain of both columns and girders, and the highest error can be found in columns in 3-D analysis for full-scale of Takatori wave. On the other hand, the analysis result of columns in 3-D with 0.4-scale wave is similar to that of experiment. Besides this, looking back the result of maximum story shear force shown in Figure 5.3(a) as well as the maximum drift angle in Figure 5.5(a), it is implied that the analysis result were higher than the experimental result due to the much higher maximum shear force in analysis (solid line) than experiment (dotted line) on 1st story for full- scale of Takatori wave.

The girder strain for 0.4-scale wave has higher value in analysis than experiment result, while it is less for full-scale wave. This is accountable by studying the result of maximum story shear represented in Figure 5.3(b), having that has the same correlation between analysis and experimental result.

Finally, we reported that the analysis results in 2-D have few discrepancies with the results in 3-D that are shown in this paper. The experimental results are not equivalent to the official data disclosed, but are estimated figures based upon the examination outcome in NIED site. (http://www.blind-analysis.jp/)

6. CONCLUSIONS

Reviewing the analysis model and seismic response analysis results in 2 award-winning categories (categories assigned with viscous dampers in 3-D and 2-D) in this paper, we have found useful technical tips in terms of accuracy enhancement.

1) Comparing the 1st natural period of experimental building and the one of analysis model, the former tends to be shorter than the latter. This tendency causes significant impact on the seismic response analysis result of buildings that are within short period region as for 1st natural period.
2) The viscous damper systems including brace and other components can be modeled accurately by Maxwell model. However, loose connections of the pin joint of damper need to be reduced as much as possible in order to maximize the damping force of the device as well as to improve the accuracy of the simulation.
3) The viscous damping model of the building that has comparatively short first natural period can be optimized by applying the individual modal damping and specifying mostly the same damping ratio from 1st to higher modes, provided that there isn't any dynamic interaction (radiation damping) with ground at all. Thus the model can duplicate the phenomena accurately.
4) The viscous damping of the building must be specified in accordance with the seismic input level. The damping ratio of the analysis model should be slightly less for 0.4-scale than for full-scale of Takatori wave.
5) The accuracy of 2-D simulation can be as high as 3-D by creating 2-D model from 3-D (limited to the two directional model), provided the eccentricity (of stiffness or of strength) of the building is small.

Acknowledgements:

The authors acknowledge support of Mr. Mitsuhiro Saito (Disaster Prevention Consulting Department, Kozo Keikaku Engineering Inc.), Mr. Tetsushi Inubushi (Structural Design Department, Osaka Office, Kozo Keikaku Engineering Inc.) and Ms. Eiko Kawamura (Overseas Marketing and Corporate Development Dept.) for these analyses and completing this paper, with sincere gratitude to their assistance.

References:

1)K.Kasai, Y.Ooki, M.Ishii, H.Ozaki, H.Ito, S.Motoyui T.Hikino, and E.Sato. (2008), "VALUE-ADDED 5-STORY STEEL FRAME AND ITS COMPONENTS: PART1 FULL-SCALE DAMPER TESTS AND ANALYSES," ***The 14th World Conference on Earthquake Engineering***, S17-01-013.

2)Y.Ooki, K.Kasai, S.Murata and Y.Yamazaki. (2009), "Shaking Machine Test of the Full Scale Value-Added 5-Story Steel Building: E-Defense Experimental Projects for Steel Building Part48," ***Summaries of Technical Papers of Annual Meeting Architectural Institute of Japan***, C-1, 749-750.

3)M.Yonetani, K.Kasai, Y.Ooki, H.Ito and T.Hikino. (2009), "Result of Shaking Table Test of 5-Story Steel Frame with Viscous Damper: E-Defense Experimental Projects for Steel Building Part45," ***Summaries of Technical Papers of Annual Meeting Architectural Institute of Japan***, C-1, 743-744.

First Place Award

This is to certify that

Tadamichi Yamashita
Jun Kawabata
Masayuki Ninomiya
Norikazu Sakaba
Yukimori Yanagawa

are the First Place Winners of
the E-Defense Blind Analysis Contest 2009
in the category of 2-Dimensional Analysis,
Viscous damper

December 7, 2009

National Research Institute for
Earth Science and Disaster Prevention,
Hyogo Earthquake Engineering Research Center

Masayoshi Nakashima,
Director of E-Defense

First Place Award

This is to certify that

Tadamichi Yamashita
Jun Kawabata
Masayuki Ninomiya
Masaki Shibata
Norikazu Sakaba
Yukimori Yanagawa

are the First Place Winners of
the E-Defense Blind Analysis Contest 2009
in the category of 3-Dimensional Analysis,
Viscous damper

December 7, 2009

National Research Institute for
Earth Science and Disaster Prevention,
Hyogo Earthquake Engineering Research Center

Masayoshi Nakashima,
Director of E-Defense